



Weather dependent mathematical model of photovoltaic panels

M. Belik¹

¹ Department of Power Engineering and Ecology
University of West Bohemia
Univerzitni 8, 30614 Pilsen (Czech Republic)
Phone/Fax number: +0420 376 734315, e-mail: belik4@kee.zcu.cz

Abstract. This article discusses issues of weather dependent mathematical model of photovoltaic panels. Unlike the other systems this model covers also transient phenomenon during fast weather conditions changes. These effects cause extraordinary levels of panel heating dramatically affecting the efficiency. Measurements, analysis and application of thermal features are evaluated on set of photovoltaic panels covering the most common technologies. The main contribution of this research is optimization of the mathematical model. Simulation results are compared with standard models.

Key words

thermal features of pv panels, pv panel simulation, mathematical model of pv system, VA characteristic, efficiency.

1. Introduction

Photovoltaic systems became standard component of power sources mix in the last years. Main pv systems disadvantage is direct dependency on solar activity respectively on the weather as whole. Prediction of power generation from these units is always a roulette but also prediction of particular efficiency can be very challenging task.

Large photovoltaic arrays but also small home systems could stand as either energy solution or interesting economical investment. Unfortunately the reality often does not correspond with earlier predictions and expectations. The reason is very simple. Optimistic pre design simulations dramatically exceed real service conditions.

Accurate knowledge base of local weather condition is critical point of all simulations and calculations. Global market is overloaded with many design software tools proposing definition of many technical and nature parameters. Best tools such as PV GIS or PV Syst offer connection to local weather stations suggesting best simulation results. Either these systems do not implement calculations during weather transients. These phases can

be so significant that can affect final power generation or economical benefit for more than 20%.

Punctual power generation projection became the goal of primary pv system numerical model. This model proceeded from more than 157 000 measured data recorded during 3 years on real system and covering complete operating set of electrical and non electrical parameters. The necessity of continuous data entering the computation is drawback of this system limiting its usage in similar way as above mentioned commercial systems.

Application of discontinuous data flow during fast weather changes became the task for evaluation of the model. The research focused on the thermal features definitions based on measurements on a set of real photovoltaic panels covering technologies from standard monocrystalline Si to modern CdTe and CIGS.

2. Primary Mathematical Model

157 680 records measured within 3 years on 20 kWp photovoltaic system enabled development of precious numerical model. Complete simulation process consists from input data synchronization and selection, simulation of DC part, simulation and spectral analysis of AC part. Only the DC part is important for this article.

The DC model is based on complete multidimensional array of VA characteristics measured during all working conditions. Size and structure of this array does not allow fast computations on a cheap controller. So the structure and size were obligated to be simplified. As the result the structure was transformed into one basic 3D VAI characteristic (volt-ampere-intensity) and two correction curves describing temperature and radiation spectrum variations. These components are represented as one 2D array and two 1D vectors. This new structure enables fast computations consisting from one direct addressed reading on 2D array, two direct addressed readings on 1D array and multiplication of three decimal numbers. Incomplete and sparse data complicate generation of the components.

Missing sparse elements can be simply completed using some numerical method. The shape and density of the real measured VA characteristics are the source of specific uncertainty what numerical method generates best results.

Depending on the frequency of specific conditions measurements can be represented either with a characteristic defined from 5 or 6 points or with a characteristic defined from 40 points or more. Also the certainty of the measured values opens the questions of approximation or interpolation. Correct method was selected after application of all methods and evaluation of the results with 1000 real measured values.

Algorithms applying double or cross various interpolation and approximation curves were compared with optimized surface generating algorithms. Basic VAI characteristic and both correction curves were calculated and tested independently. Applied numerical methods are summarized in Table I.

Table I. – Applied Numerical Methods

Array	C ¹ inter	C ² inter	Polyn 4	Polyn 5
VAI	yes	yes	yes	yes
t	yes	yes	yes	yes
UV	yes	yes	yes	yes
Array	B-spline	Bezier curve	Bezier surf	Spline surf
VAI	yes	yes	yes	yes
t	yes	yes	no	no
UV	yes	yes	no	no

Table II. shows random example of operating conditions used for simulations during algorithms testing.

This presented sample statistically covers typical range of real conditions for synoptical overview while total set consists from 1000 samples.

Table II. – Operating Conditions

Sample	1	2	3	4	5
I [W/m ²]	89	142	210	380	486
U [V]	236	303	267	278	322
t [°C]	14,9	28,2	27,3	30,1	33,4
UV [W/m ²]	230	240	280	310	290
Sample	6	7	8	9	10
I [W/m ²]	616	722	839	948	1043
U [V]	273	290	320	267	263
t [°C]	39,7	14,8	44,6	38,2	45,6
UV [W/m ²]	320	240	300	260	270

Application of all methods on the presented example and simulated output current variances compared with real measured data are displayed in Table III.

Table III. – Variances of the Methods

Sample	1	2	3	4	5
Iout [A]	0,79	1,07	1,83	3,46	4,39
C1 interpol [A]	0,77	1,08	1,86	3,39	4,41
C2 interpol [A]	0,77	1,12	1,73	3,41	4,33
Polynom 4 [A]	0,83	1,11	1,88	3,36	4,26
Polynom 5 [A]	0,78	1,11	1,86	3,51	4,47
B-spline [A]	0,81	1,13	1,92	3,41	4,29
Bézier curve [A]	0,82	1,01	1,88	3,53	4,46
Bézier surface [A]	0,76	1,01	1,91	3,28	4,51
spline surface [A]	0,77	1,10	1,89	3,36	4,48
Sample	6	7	8	9	10
Iout [A]	5,41	6,63	7,31	8,24	9,09
C1 interpol [A]	5,53	6,48	7,13	8,01	9,22
C2 interpol [A]	5,49	6,51	7,37	8,16	9,17
Polynom 4 [A]	5,35	6,47	7,18	8,35	8,96
Polynom 5 [A]	5,36	6,53	7,22	8,34	9,14
B-spline [A]	5,32	6,69	7,41	8,31	9,01
Bézier curve [A]	5,48	6,73	7,10	8,33	9,21
Bézier surface [A]	5,29	6,82	7,39	8,36	8,97
spline surface [A]	5,30	6,66	7,26	8,09	9,13

Final variation percentage and statistical error margins calculated from the complete 1000 sample set are presented in Table IV.

Table IV. – Final Variations and Margins

Sample	1	2	3	4	5	6
C1 interpol [%]	2,53	1,93	2,64	2,02	1,46	2,22
C2 interpol [%]	2,53	0,96	5,46	1,45	1,37	2,48
Polynom 4 [%]	5,06	1,87	2,73	2,89	2,96	1,11
Polynom 5 [%]	1,27	1,87	2,64	2,45	2,82	1,92
B-spline [%]	2,53	1,93	4,92	1,45	2,28	1,66
Bézier curve [%]	3,80	2,80	2,73	2,02	1,59	1,29
Bézier surface [%]	3,80	1,87	2,37	5,20	2,73	2,22
spline surface [%]	2,53	2,80	3,28	2,89	2,05	2,03
Sample	7	8	9	Min	Max	Ave.
C1 interpol [%]	2,26	2,46	2,79	0,26	6,11	2,87
C2 interpol [%]	1,81	1,82	1,97	0,23	5,98	2,77
Polynom 4 [%]	2,41	1,78	2,33	0,21	5,99	2,36
Polynom 5 [%]	1,51	2,23	1,21	0,18	6,01	2,35
B-spline [%]	0,90	1,37	0,85	0,31	5,84	2,18
Bézier curve [%]	1,51	2,87	1,09	0,31	6,02	2,22
Bézier surface [%]	2,87	1,09	1,46	0,33	5,93	2,19
spline surface [%]	0,45	0,68	1,82	0,32	5,81	2,06

All applied methods returned values with error in the range between 0,21 and 6,11 % what did not favouritism any of them. Method of spline surface was selected for the VAI array because of well optimized and efficient algorithm while t and UV correction curves were

computed using the most simple, but for this case enough accurate, 4th degree polynomial algorithm.

Fig. 1. shows graphical representation of the bicubic spline surface interpolation for the basic VAI array. Fig. 2. displays the shape of UV correction curve while Fig. 3. presents of t correction curve, visualized results of the 4th degree polynomial interpolation.

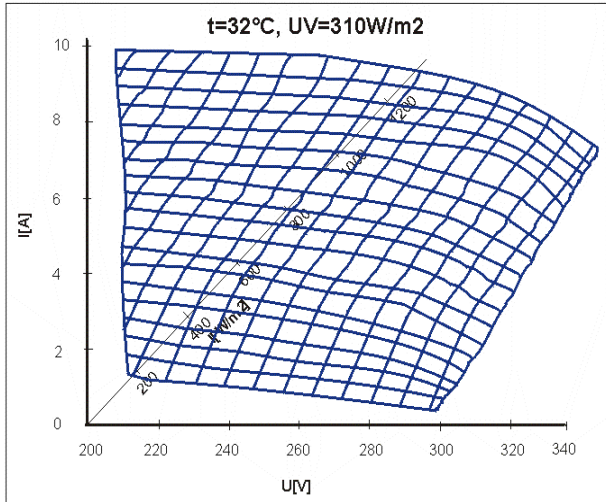


Fig. 1. VAI array of the numerical model.

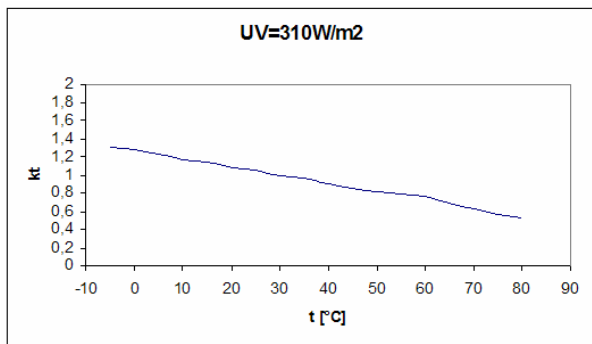


Fig. 2. UV correction curve of the numerical model.

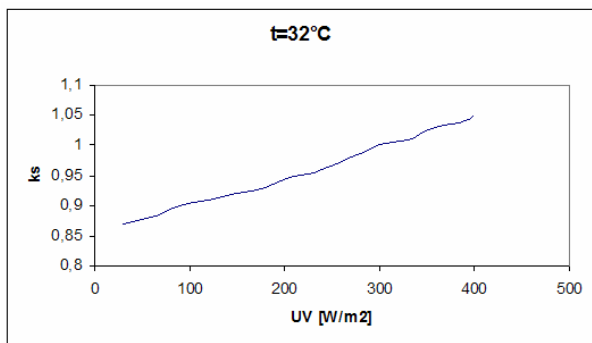


Fig. 3. t correction curve of the numerical model.

Fig. 1, Fig. 2 and Fig. 3 also demonstrate the definition conditions for the model. It is evident that these conditions does not correspond with the definition of the Standard Test Conditions (STC).

Definition temperature $t = 32^{\circ}\text{C}$ and definition spectral composition $UV = 310 \text{ W/m}^2$ were selected from practical reasons. Dataset for these conditions was the most

complete and the most compact so that also calculated VAI array is the most accurate. STC parameters can be easily recalculated from the t and UV correction curves.

3. Weather Correction of the Model

Continuity of the input (measured) data evokes practical limits for real application of the presented numerical model.

Original data are recorded and logged with the period of 10 min. This sampling period is practical for storage and global overview but is not accurate enough for energy production calculation or prediction.

The 10 min period is very long if we focus on the solar radiation intensity itself. Fig. 4 presents measured radiation incidenting surface of a real PV cell and Fig. 5 demonstrates measured temperature of that cell. Typical winter sunny day is symbolized with blue color while pink color illustrates typical winter cloudy day.

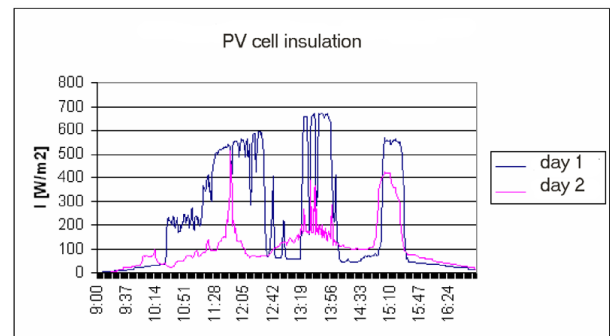


Fig. 4. insulation of measured PV cell.

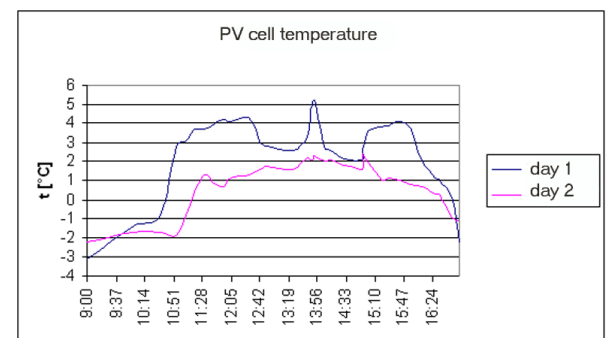


Fig. 5. temperature of measured PV cell.

Strong oscillations and drops in the solar intensity chart are flatten in the temperature diagram.

Measurements proved that the temperature strongly depends on the intensity and the type of the panel. Influence of the other ambient conditions such as air temperature, humidity and wind speed and direction is during short periods only marginal.

From the mathematical point of view we can find temperature trends that are depending on 2 intensity levels as variables, on a constant representing type of the

panel and on starting temperature as the boundary condition.

Thermal characteristics of a set consisting from mono Si and poly Si glass panels, CIGS glass and flexi panels, CdTe glass panel and organic flexi panel were measured. Fig. 6 presents sample VA characteristics of sample panel measured during different conditions. Number of the curves does not enable clear identification and labeling but the cardinal changes of the characteristics are evident. Also changes of the Maximum Power Point and Fill Factor can be simply traced.

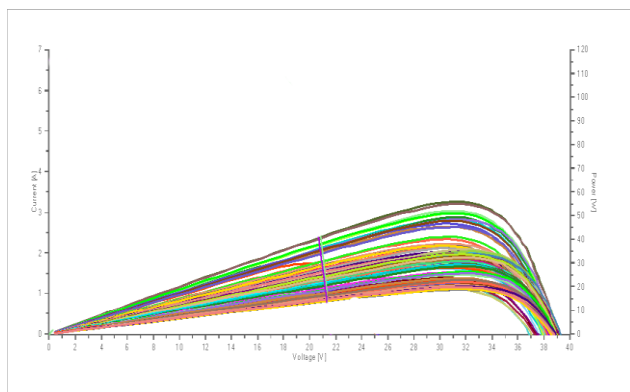


Fig. 6. Measured sample VA characteristics (not labeled).

Two way measurements were separately executed. Firstly, each cool panel was installed in insulated position and the heating process was started. Actual temperature and VA characteristic were recorded in sufficient time interval. This interval is not constant but depends on the panel. While the panel reached maximum temperature, it was reinstalled into original shaded position. Again the temperatures and VA characteristics were logged throughout all the inverse cooling process.

Analyser HT Solar IV-400 with auxiliary radiation and temperature sensor was used for these measurements. Table V demonstrates representative set of testing conditions.

Table V. – Testing Conditions

	1	2	3	4	5
T_{SHADE} (°C)	-5,1	1,7	12,3	20,5	28,4
T_{SUN} (°C)	0,5	12,5	23,6	29,4	36,2
I_{SHADE} (W/m²)	86	97	118	139	156
I_{SUN} (W/m²)	351	423	567	745	921
Humidity (%)	80	83	86	74	76
Wind_{speed}(m/s)	0,6	0,7	3,6	4,5	3,5
Wind_{direction} (°)	NNW	NWN	WWS	WWS	WSS

All measurements were doubled in dead air area to exclude influence of wind cooling, but this process tends in short periods to only marginal contribution.

Table VI demonstrates final temperature of heating process and elapsed time before reaching maximal and

minimal temperature at irradiation 300, 500 and 800 W/m² while Fig. 7 displays features of thermal coefficient during heating and cooling process of selected panels.

Table VI. – Heating and Cooling Process

	Si-m glass	Si-p glass	CIGS glass	CIGS flexi	CdTe glass
T₃₀₀ MAX (°C)	8,2	8,4	7,3	5,5	8,4
T₅₀₀ MAX (°C)	20,5	21,5	19,6	19,4	20,2
T₈₀₀ MAX (°C)	46,1	45,7	44,8	41,9	45,6
t₃₀₀ heat (s)	384	379	401	512	417
t₃₀₀ cool (s)	464	491	508	710	479
t₅₀₀ heat (s)	316	321	325	374	316
t₅₀₀ cool (s)	399	398	410	643	419
t₈₀₀ heat (s)	212	215	216	254	215
t₈₀₀ cool (s)	294	295	287	544	295

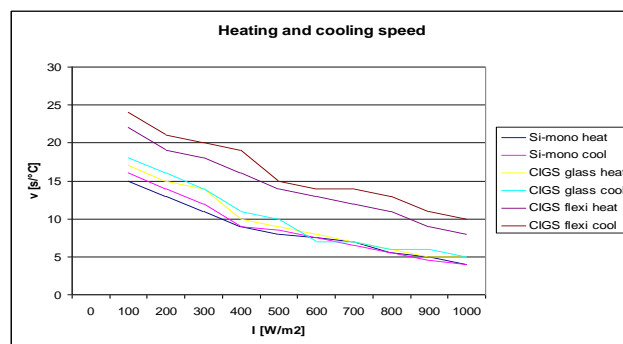


Fig. 7. Heating and cooling speed of the panels.

4. Results and Conclusions

The measurement results have shown that the heating process is much faster for all panel types than the cooling process except the organic flexi panel. Surface structure of the covering film caused that the heating was in this case a bit slower than the cooling. The glass panels disclosed higher thermal capacity and slower heat transfer than the flexi panels. Higher radiation intensities caused faster heating than lower intensities even if the temperature difference was equal.

Implementation of the thermal coefficient into the model improves range of application while the accuracy of the computation stays at the same level with average variance 2,16 %.

References

- [1] Kunovsky J, Modern Taylor Series Method, IEEE 13th ISCI, Poprad 2015.
- [2] Kunovsky J, Construction of P1 Gradient from P0 by Averaging, 12th ICNAAM. Rhodes 2014.
- [3] Cihelka, Solarni tepelna tehnika, T. Malina, Praha, 1994.
- [4] M. Libra, V. Poulek, Solarni energie, CZU, Praha, 2005.